1

General introduction

In the 1980s the first successful experiments [312] and theory [98], demonstrating that light could be used to cool and confine atoms to submillikelvin temperatures, opened several exciting new chapters in atomic, molecular, and optical (AMO) physics. Atom interferometry [6, 8], matter–wave holography [294], optical lattices [192], and Bose–Einstein condensation in dilute gases [18, 95] all exemplified significant new physics where collisions between atoms cooled with light play a pivotal role. The nature of these collisions has become the subject of intensive study not only because of their importance to these new areas of AMO physics but also because their investigation has led to new insights into how cold collision spectroscopy can lead to precision measurements of atomic and molecular parameters and how radiation fields can manipulate the outcome of a collision itself. As a general orientation Fig. 1.1 shows how a typical atomic de Broglie wavelength varies with temperature and where various physical phenomena situate along the scale. With de Broglie wavelengths on the order of a few thousandths of a nanometer, conventional gas-phase chemistry can usually be interpreted as the interaction of classical nuclear point particles moving along potential surfaces defined by their associated electronic charge distribution. At one time liquid helium was thought to define a regime of cryogenic physics, but it is clear from Fig. 1.1 that optical and evaporative cooling have created "cryogenic" environments below liquid helium by many orders of magnitude. At the level of Doppler cooling and optical molasses[1] the de Broglie wavelength becomes comparable to or longer than the chemical bond, approaching the length of the cooling optical light wave. Here we can expect wave and relativistic effects such as resonances, interferences, and interaction retardation to become important. Following Suominen [370], we will term the Doppler cooling and optical molasses temperature range [407], roughly between 1 mK and 1 μK, the regime of cold collisions. Most collision phenomena at this level are studied in the presence of one or more light fields used to confine the atoms and to probe their interactions. Excited quasimolecular states often play an important role. Below about 1 μK, where evaporative cooling and

[1] A good introduction to the early physics of laser cooling and trapping can be found in two special issues of the *Journal of the Optical Society of America* B. These are: The mechanical effects of light, *J. Opt. Soc. Am.* B **2,** No. 11, November 1985 and Laser cooling and trapping of atoms, *J. Opt. Soc. Am.* B **6,** No. 11, November 1989. Two more recent reviews [7, 271] update a decade of developments since the early work recounted in the *J. Opt. Soc. Am.* B special issues.

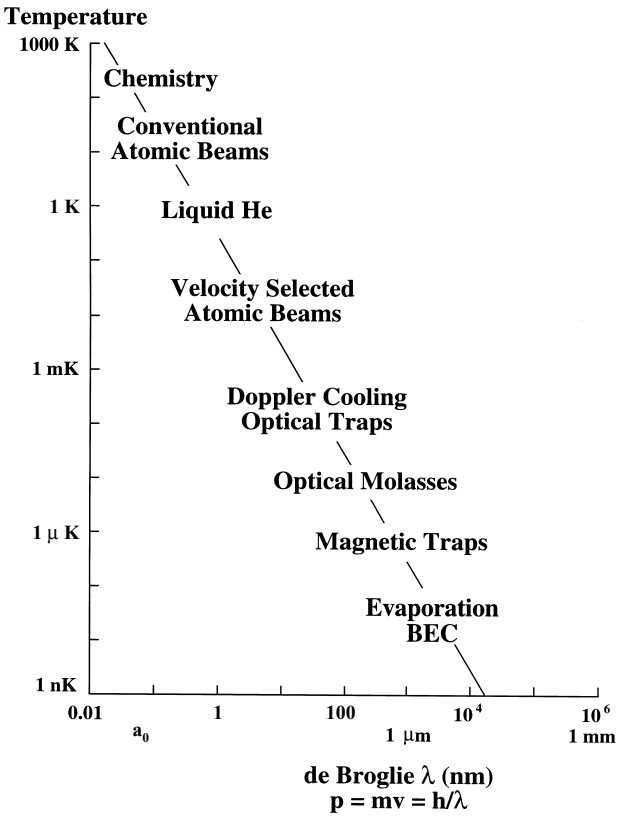

Fig. 1.1. Illustrative plot of various physical phenomena along a scale of temperature (energy divided by Boltzmann's constant k_B) plotted against the de Broglie wavelength for atomic sodium.

Bose–Einstein condensation[2] (BEC) become the focus of attention, the de Broglie wavelength grows to a scale comparable to the mean distance separating atoms at the critical condensation density; quantum degenerate states of the atomic ensemble begin to appear. In this regime ground-state collisions only take place through radial (not angular) motion and are characterized by a phase shift, or scattering length, of the ground-state wavefunction. Since the atomic translational energy now lies below the kinetic energy transferred to an atom by recoil from a scattered photon, light can play no role; and collisions occur in a temperature range from 1 μK $\rightarrow$ 0 and in the dark. These collisions are termed ultracold. The terms "cold" and "ultracold" have been used in various ways in the past but now we adopt the terminology of Suominen [370] in distinguishing between the two. This book will recount progress in understanding collision processes in both the cold and ultracold domains.

[2] For an introduction to research in alkali-atom Bose–Einstein condensation see the special issue on Bose–Einstein condensation in the *Journal of Research of the National Institute of Standards and Technology* **101,** No. 4, July–August 1996.

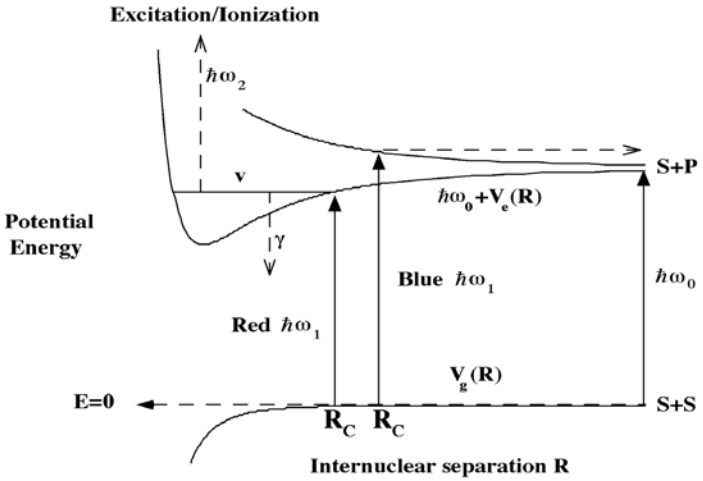

Fig. 1.2. Schematic of a cold collision. Light field $\hbar\omega_1$, red detuned with respect to the S + P asymptote, excites the quasimolecule in a free–bound transition around the Condon point R_C and can lead to excitation or ionization with the absorption of a second photon $\hbar\omega_2$. Light field $\hbar\omega_1$, blue detuned with respect to the S + P asymptote, prevents atoms from approaching significantly beyond the Condon point. Blue-detuned excitation leads to optical shielding and suppression of inelastic and reactive collision rates.

We start with cold collisions because many experiments carried out in optical traps and optically slowed atomic beams take place in this temperature range. In 1986, soon after the first successful experiments reported optical cooling and trapping in alkali gasses, J. Vigué published a paper discussing the possible consequences of binary collisions in a cold or ultracold gaseous medium [415]. Figure 1.2 shows schematically the general features of a cold binary collision. Two S ground-state atoms interact at long range through electrostatic dispersion forces, and approach along an attractive C_6/R^6 potential. The first excited states, correlating to an S + P asymptote and separated from the ground state by the atomic excitation energy $\hbar\omega_0$, interact by resonance dipole–dipole forces and approach either along an attractive or repulsive C_3/R^3 curve. If the colliding atoms on the ground-state potential encounter a *red-detuned* optical field $\hbar\omega_1$, the probability of a free–bound transition to some vibration–rotation level v of the attractive excited state will maximize around the Condon point R_C, where $\hbar\omega_1$ matches the potential difference. The quasimolecule finds itself photoassociated and vibrating within the attractive well. A second field $\hbar\omega_2$ can then further excite or even ionize the photoassociated quasimolecule, or it can relax back to some distribution of the continuum and bound levels of the ground state with a spontaneous emission rate Γ. Photoassociation and subsequent inelastic processes comprise the discussion of Chapters 4 and 5. If the atoms colliding on the ground-state potential interact with a *blue-detuned* optical field $\hbar\omega$, the probability of transition to some continuum level of the repulsive excited state will maximize around the Condon point R_C, which will also be quite close to the turning point of the nuclear motion on the repulsive excited state. The atoms approach no further and begin to separate along the repulsive curve leading to the

S + P asymptote. The blue-detuned field "shields" the atoms from further interaction at more intimate internuclear separation and "suppresses" the rate of various inelastic and reactive processes. Optical shielding and suppression is the topic of Chapter 6. Cold collisions in the presence of optical fields or in the ground state reveal new physics in domains where atomic scales of length, time, and spectral line width are reversed from their conventional relations. In addition to the atomic de Broglie wave increasing to a length several hundred times that of the chemical bond, the collisional interaction time grows to several times the spontaneous emission lifetime, and the inhomogeneous Doppler line width at cold and ultracold temperatures narrows to less than the natural width of an atomic dipole transition. The narrow, near-threshold continuum state distribution means that at most a few partial waves will contribute to a scattering event. Averaging therefore does not obscure matter wave effects such as resonances, nodes and antinodes in scattering wavefunction amplitudes, and channel-opening threshold laws. In the cold collision regime, Doppler broadening is narrow compared to the radiative natural width; and therefore permits ultrahigh-precision, free–bound molecular spectroscopy and efficient participation of the entire atom ensemble in the excitation process. Long collision duration ensures interacting partners sufficient time to exchange multiple photons with modes of an externally applied radiation field. The frequency, intensity, and polarization of the optical field can in turn modify effective interaction potentials and control the probability of inelastic, reactive, and elastic final product channels.

Three questions have motivated significant developments in cold collisions:

(1) How do collisions lead to loss of atom confinement in traps?
(2) How can photoassociation spectroscopy yield precision measurements of atomic properties and insight into the quantum nature of the scattering process itself?
(3) How can optical fields be used to control the outcome of a collisional encounter?

This third question has had an enduring appeal to chemical physicists, and we review here some of the early history to put current developments in perspective and to emphasize the importance of the ultracold regime. In the decade of the 1970s, after the development of the CO_2 laser, researchers in atomic and chemical physics immediately thought to use it to influence or control inelastic processes and chemical reaction. However, early attempts to induce reactivity by exciting well-defined, localized molecular sites such as double bonds or functional groups failed because the initial optical excitation diffused rapidly into the rotations, vibrations, and torsional bending motions of the molecular nuclei. The unfortunate result was that the infrared light of the CO_2 laser essentially heated the molecules much as the familiar and venerable Bunsen burner. Enthusiasm for laser-controlled chemistry cooled when researchers realized that this rapid energy diffusion throughout the molecular skeleton blocked significant advance along the road to optical control of reactivity. In the early 1980s the development of the pulsed dye laser, tunable in the visible region of the spectrum, together with new proposals for "radiative collisions," in which the electrons of the molecule interact with the light rather than the nuclei, revived interest. A second round of experiments achieved some success in optically transforming reactants to products; but in general the high peak powers necessary to enhance reactivity significantly interfered

with the desired effects by inducing nonlinear, multiphoton excitation and ionization in the molecule itself. The necessity for high peak power in turn arose from two crucial factors: (1) Doppler broadening at ambient temperature permits only a few per cent of all molecular collisions to interact with an applied optical field mode so the product "yield" is low, and (2) the optical field had to influence the strong chemical binding interaction in order to affect atomic behavior during the collisional encounter. This requirement implied the need for power densities greater than a few megawatts per square centimeter. Power densities of this order are well above the threshold for multiphoton absorption and ionization, and these processes quickly convert atoms or molecules from a neutral gas into an ionized plasma. It appeared depressingly difficult to control collisions with light without first optically destroying them.

However, atomic deceleration and optical cooling brightened this discouraging picture, by narrowing the inhomogeneous Doppler broadening to less than a natural line width of an atomic transition and transferring the optical–particle interaction from the "chemical" zone of strong wavefunction overlap to an outer region where weak electrostatic terms characterize the collision. In this weakly interacting outer zone only hundreds of milliwatts per square centimeter of optical power density suffice to profoundly alter the inelastic and reactive collision rate constant. Furthermore, although a conventional atomic collision lasts only a few hundred femtoseconds, very short compared to the tens of nanoseconds required before excited molecules or atoms spontaneously emit light, in the ultracold regime particles move much more slowly, taking up to hundreds of nanoseconds to complete a collisional encounter. The long collision duration leaves plenty of time for the two interacting partners to absorb energy from an external radiation field or to emit energy by spontaneous or stimulated processes.

To the three earlier questions motivating studies of cold collisions may now be added a fourth relevant to the ultracold regime: what role do collisions play in the attainment and behavior of boson and fermion gases in the quantum degenerate regime? Quantum statistical effects have been observed and studied in the superfluidity of liquid helium and in the phenomena of metallic and high-temperature superconductivity. These dramatic and significant manifestations of quantum collective effects, are nevertheless difficult to study at the atomic level because the particles are condensed and strongly interacting. Observation and measurement in weakly interacting dilute gases, however, relate much more directly to the simplest, microscopic models of this behavior. The differences between model "ideal" quantum gases and "real" quantum gases begin with binary interactions between the particles, and therefore the study of ultracold collisions is a natural point of departure for investigation. Collisions determine two crucial aspects of BEC experiments: (1) the evaporative cooling rate necessary for the attainment of BEC depends on the elastic scattering cross section, proportional to the square of the s-wave scattering length, and (2) the sign of the scattering length indicates the stability of the condensate: positive scattering lengths lead to large stable condensates while negative scattering lengths do not. The ability to produce condensates by sympathetic cooling also depends critically on the elastic and inelastic (loss and heating) rate constants among different states of the colliding partners. Although a confined Bose atom condensate bears some analogy to an optical cavity (photons are bosons),

the atoms interact through collisions; and these collisions limit the coherence length of any "atom laser" coupled out of the confining "cavity" or BEC trap. Another important point, relating back to optical control, is that the amplitude and sign of the scattering length depends sensitively on the fine details of the ground potentials. The possibility of manipulating these potentials and consequently collision rates with external means, using optical, magnetic, or radio-frequency fields, holds the promise of tailoring the properties of the quantum gas to enhance stability and coherence. Finally it now appears that the limiting loss process for dilute gaseous Bose–Einstein condensates are three-body collisions that also measure the third-order coherence, thus providing a critical signature of true quantum statistical behavior. Understanding the quantum statistical collective behavior of ultracold dilute gases will drive research in ultracold collisions for years to come.

2

Introduction to cold collision theory

2.1 Basic concepts of scattering theory

Let us first consider some of the basic concepts that are needed to describe the collision of two ground-state atoms. We initially consider the collision of two distinguishable, structureless particles a and b with interaction potential $V_g(R)$ moving with relative momentum $\mathbf{k}$, where $\mathbf{R}$ is the vector connecting a and b. We will generalize below to the cases of identical particles and particles with internal structure. The collision energy is

$$E = \frac{\hbar^2 k^2}{2\mu},$$

where μ is the reduced mass of the two particles. If there is no interaction between the particles, $V_g = 0$, the wavefunction describing the relative motion of the two particles in internal states $|0_a\rangle$ and $|0_b\rangle$ is

$$\Psi_g^+(\mathbf{R}) = \mathrm{e}^{\mathrm{i}\mathbf{k}\cdot\mathbf{R}}|0_a 0_b\rangle. \tag{2.1}$$

If the interaction potential is nonzero, the collision between the particles results in a scattered wave, and at large R beyond the range of the potential the wavefunction is represented as

$$\Psi_g^+(\mathbf{R}) \sim \left[\mathrm{e}^{\mathrm{i}\mathbf{k}\cdot\mathbf{R}} + \frac{\mathrm{e}^{\mathrm{i}kR}}{R} f(E, \hat{\mathbf{k}}, \hat{\mathbf{k}}_\mathbf{s})\right]|0_a 0_b\rangle, \tag{2.2}$$

where $\hat{\mathbf{k}}$ is a unit vector indicating the direction of $\mathbf{k}$ and $\hat{\mathbf{k}}_\mathbf{s}$ is a unit vector indicating the direction of the scattered wave with amplitude $f(E, \hat{\mathbf{k}}, \hat{\mathbf{k}}_\mathbf{s})$. The overall effect of the collision is described by a cross section $\sigma(E)$. In a gas cell, for which all directions $\hat{\mathbf{k}}$ are possible, $\sigma(E)$ is determined by integrating over all scattered directions and averaging over all values of initial $\hat{\mathbf{k}}$:

$$\sigma(E) = \int_{4\pi} \frac{\mathrm{d}\hat{\mathbf{k}}}{4\pi} \int_{4\pi} \mathrm{d}\hat{\mathbf{k}}_\mathbf{s}\, |f(E, \hat{\mathbf{k}}, \hat{\mathbf{k}}_\mathbf{s})|^2. \tag{2.3}$$

Since f has units of length, the cross section has units of length^2 = area. Equation 2.3 simplifies for a spherically symmetric potential, for which f depends only on the angle θ

between $\hat{\mathbf{k}}$ and $\hat{\mathbf{k}}_\mathbf{s}$:

$$\sigma(E) = 2\pi \int_0^\pi \mathrm{d}\theta \sin(\theta) |f(E,\theta)|^2. \tag{2.4}$$

The object of scattering theory is to calculate the scattering amplitude and cross section, given the interaction potentials between the two atoms. The first step in reducing the problem to practical computation is to introduce the partial wave expansion of the plane wave:

$$\mathrm{e}^{\mathrm{i}\mathbf{k}\cdot\mathbf{R}} = 4\pi \sum_{\ell=0}^{\infty} \sum_{m=-\ell}^{\ell} \mathrm{i}^\ell Y^*_{\ell m}(\hat{\mathbf{k}}) Y_{\ell m}(\hat{\mathbf{k}}_\mathbf{s}) j_\ell(kR), \tag{2.5}$$

where $Y_{\ell m}$ is a spherical harmonic and the function j_ℓ has the following form as $R \to \infty$:

$$j_\ell(kR) \sim \frac{\sin\left(kR - \frac{\pi}{2}\ell\right)}{kR}. \tag{2.6}$$

The complete wavefunction at all R is also expanded in a partial wave series:

$$\Psi_g^+(\mathbf{R}) = 4\pi \sum_{\ell=0}^{\infty} \sum_{m=-\ell}^{\ell} \mathrm{i}^\ell Y^*_{\ell m}(\hat{\mathbf{k}}) Y_{\ell m}(\hat{\mathbf{k}}_\mathbf{s}) \frac{F_\ell^+(E,R)}{R} |0_a 0_b\rangle, \tag{2.7}$$

where $F_\ell^+(E,R)$ is determined from the Schrödinger equation,

$$\frac{\mathrm{d}^2 F_\ell^+(E,R)}{\mathrm{d}R^2} + \frac{2\mu}{\hbar^2}\left[E - V_g(R) + \frac{\hbar^2 \ell(\ell+1)}{2\mu R^2}\right] F_\ell^+(E,R) = 0. \tag{2.8}$$

By imposing the following boundary condition on $F_\ell^+(E,R)$ as $R \to \infty$, the asymptotic wavefunction has the desired form, Eq. 2.2, representing an incident plane wave plus a scattered wave:

$$\frac{F_\ell^+(E,R)}{R} \sim \sin\left(kR - \frac{\pi}{2}\ell + \eta_\ell\right) \frac{\mathrm{e}^{\mathrm{i}\eta_\ell}}{kR} \tag{2.9}$$

$$\sim j_\ell(kR) + \frac{\mathrm{i}}{2} \frac{\mathrm{e}^{\mathrm{i}(kR - \frac{\pi}{2}\ell)}}{kR} T_\ell(E). \tag{2.10}$$

Here η_ℓ is the phase shift induced by the interaction potential $V_g(R)$, and $T_\ell(E) = 1 - \mathrm{e}^{2\mathrm{i}\eta_\ell}$ is the T-matrix element from which the amplitude of the scattered wave is determined,

$$f(E, \hat{\mathbf{k}}, \hat{\mathbf{k}}_\mathbf{s}) = \frac{2\pi\mathrm{i}}{k} \sum_{\ell=0}^{\infty} \sum_{m=-\ell}^{\ell} \mathrm{i}^\ell Y^*_{\ell m}(\hat{\mathbf{k}}) Y_{\ell m}(\hat{\mathbf{k}}_\mathbf{s}) T_\ell(E). \tag{2.11}$$

Using the simpler form of Eq. 2.4, the cross section becomes

$$\sigma(E) = \frac{\pi}{k^2} \sum_{\ell=0}^{\infty} (2\ell+1) |T_\ell(E)|^2 \tag{2.12}$$

$$= \frac{4\pi}{k^2} \sum_{\ell=0}^{\infty} (2\ell+1) \sin^2 \eta_\ell. \tag{2.13}$$

The cross section has a familiar semiclassical interpretation. If the interaction potential $V_g(R)$ vanishes, the particle trajectory is a straight line with relative angular momentum $\mathbf{R} \times \mathbf{p} = bp$, where p is linear momentum and b is the distance of closest approach. If we take the angular momentum to be

$$bp = \hbar\sqrt{\ell(\ell+1)} \approx \hbar\left(\ell + \frac{1}{2}\right),$$

where the "classical" ℓ here is not quantized, then b is the classical turning point of the repulsive centrifugal potential $\hbar^2\ell(\ell+1)/2\mu R^2$ in Eq. 2.8. The semiclassical expression for the cross section, analogous to Eq. 2.12, has the form of an area,

$$\sigma(E, \text{semiclassical}) = 2\pi \int_0^\infty bP(b, E)\, db \tag{2.14}$$

weighted by $P(b, E) = |T_\ell(E)|^2$. An important feature of cold collisions is that only a very few values of ℓ can contribute to the cross section, because the classical turning points of the repulsive centrifugal potential are at large values of R. Only collisions with the very lowest ℓ values allow the atoms to get close enough to one another to experience the interatomic interaction potential. We will discuss below the specific quantum properties associated with discrete values of ℓ. Semiclassical theory is useful for certain types of trap loss collisions in relatively warm traps where light is absorbed by atom pairs at very large R, but a quantum treatment always becomes necessary at sufficiently low collision energy.

In the simple introduction above, the cross section in Eq. 2.13 represents elastic scattering, for which the internal states of the particles do not change, and their relative kinetic energy E is the same before and after the collision. In general, the atoms will have nonzero internal angular momentum due to hyperfine structure in the case of alkali atoms or due to electronic structure in the case of rare gas metastable atoms. In a field-free region, these internal states are characterized by total angular momentum F and projection M on a space-fixed quantization axis. Often an external field, either a magnetic, optical, or radio-frequency electromagnetic field, is present in cold collision experiments; and these FM states are modified by the external field. Species such as hydrogen and alkali atoms, which have ^{2}S ground states and nonvanishing nuclear spin I, have two hyperfine components with $F = I + \frac{1}{2}$ and $F = I - \frac{1}{2}$. Figure 2.1 shows the Zeeman splitting of the two $F = 1$ and $F = 2$ hyperfine components of ground-state ^{87}Rb atoms, and Fig. 2.2 shows the ground-state interaction potentials for two interacting Rb atoms. If the atomic field-modified states, commonly called field-dressed states, are represented by $|\alpha_i\rangle$ for atom $i = a, b$, then the general collision process represents a transition from the state $|\alpha_a\rangle\,|\alpha_b\rangle$ to the state $|\alpha'_a\rangle|\alpha'_b\rangle$, represented by the general transition amplitude

$$f(E, \hat{\mathbf{k}},\ \hat{\mathbf{k}}_\mathbf{s}, \alpha_a\alpha_b \rightarrow \alpha'_a\alpha'_b)$$

and the T-matrix element

$$T(E, \alpha_a\alpha_b \rightarrow \alpha'_a\alpha'_b).$$

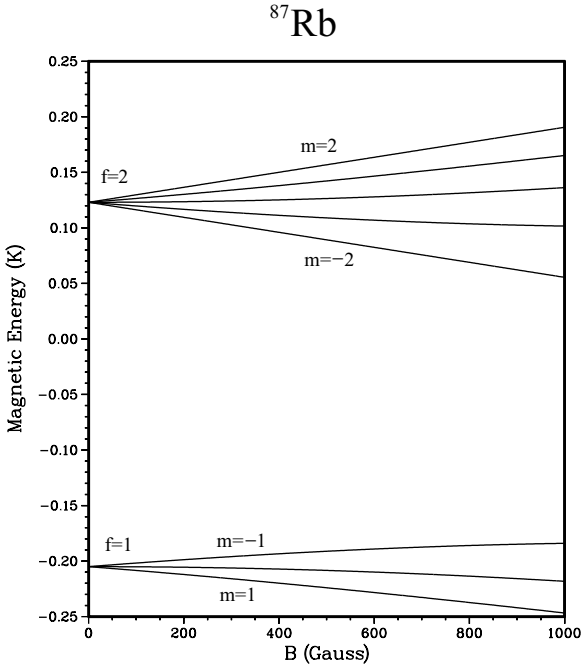

Fig. 2.1. Ground hyperfine levels of the ^{87}Rb atom versus magnetic field strength. The Zeeman splitting manifolds are evident. The energy has been divided by the Boltzmann constant in order to express it in temperature units.

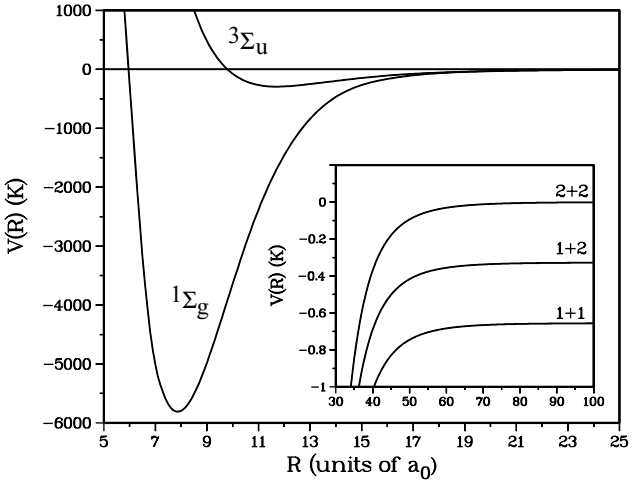

Fig. 2.2. The ground-state potential energy curves of the Rb_2 molecule. The potentials have been divided by the Boltzmann constant in order to express them in units of temperature. The full figure shows the short-range potentials on the scale of chemical bonding. The inset shows a blowup at long range, showing the separated atom hyperfine levels $F_a + F_b = 1 + 1, 1 + 2$, and $2 + 2$. The upper two potentials in the inset correlate adiabatically with $^3\Sigma_u$.